

2010

# Vibrational spectroscopic monitoring of CO<sub>2</sub>-O energy transfer: cooling processes in atmospheres of Venus & Mars

Jakob Aaron Schaeffer  
*Bucknell University*

Follow this and additional works at: [https://digitalcommons.bucknell.edu/honors\\_theses](https://digitalcommons.bucknell.edu/honors_theses)



Part of the [Physics Commons](#)

---

## Recommended Citation

Schaeffer, Jakob Aaron, "Vibrational spectroscopic monitoring of CO<sub>2</sub>-O energy transfer: cooling processes in atmospheres of Venus & Mars" (2010). *Honors Theses*. 29.  
[https://digitalcommons.bucknell.edu/honors\\_theses/29](https://digitalcommons.bucknell.edu/honors_theses/29)

This Honors Thesis is brought to you for free and open access by the Student Theses at Bucknell Digital Commons. It has been accepted for inclusion in Honors Theses by an authorized administrator of Bucknell Digital Commons. For more information, please contact [dcadmin@bucknell.edu](mailto:dcadmin@bucknell.edu).

VIBRATIONAL SPECTROSCOPIC MONITORING OF CO<sub>2</sub>-O ENERGY TRANSFER:

COOLING PROCESSES IN THE ATMOSPHERES

OF VENUS & MARS

by

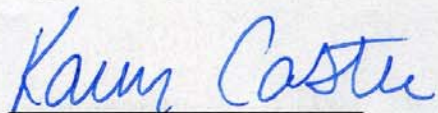
**Jakob A. Schaeffer**

A Proposal Submitted to the Honors Council

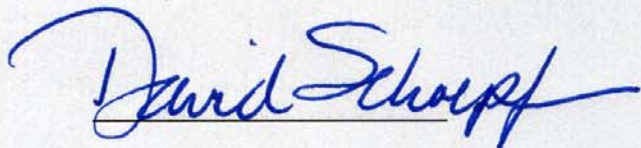
For Honors in Physics & Astronomy

04/21/10

Approved by:

Handwritten signature of Karen Castle in blue ink.

Advisor: Karen Castle

Handwritten signature of David Schoepf in blue ink.

Dept. Chair: David Schoepf

**Acknowledgements**

I'd like to thank Professor Karen Castle for her wonderful support in this endeavor as well as the help of Labe Black, Tara Pedersen, Stephen Ragard and Tricia Clyde in the lab. Also many thanks to my family, friends and all those wonderful people out there in the dark<sup>1</sup>.

**Table of Contents**

Acknowledgements.....	iv
Table of Contents.....	v
List of Figures.....	vi
Abstract.....	vii
Thesis: VIBRATIONAL SPECTROSCOPIC MONITORING OF CO <sub>2</sub> -O ENERGY TRANSFER: COOLING PROCESSES IN THE ATMOSPHERES OF VENUS & MARS.....	1
Bibliography.....	12

**List of Figures**

Figure 1 : Experimental set-up schematic.....	4
Figure 2 : Vibrational energy levels for $^{12}\text{CO}_2$ & $^{13}\text{CO}_2$ .....	5
Figure 3 : Diode beam-path schematic.....	6
Figure 4 : Fitted transient absorption curve.....	7
Figure 5 : Observed and HITRAN spectrum for $^{13}\text{CO}_2$ .....	8
Figure 6 : Vibrational spectrum of $^{13}\text{CO}_2$ with increasing $^{13}\text{CO}_2$ flow rate.....	9
Figure 7 : Plot of $(10^0)$ $^{13}\text{CO}_2$ -O VET rate as a function of O atom concentration.....	10
Figure 8 : Transient curve and fit for $(10^0)$ $^{13}\text{CO}_2$ -O quenching at given [O].....	11

## Abstract

The vibrational excitation of CO<sub>2</sub> by a fast-moving O atom followed by infrared emission from the vibrationally excited CO<sub>2</sub> has been shown to be an important cooling mechanism in the upper atmospheres of Venus, Earth and Mars. We are trying to determine more precisely the efficiency (rate coefficient) of the CO<sub>2</sub>-O vibrational energy transfer. For experimental ease the reverse reaction is used, *i.e.* collision of a vibrationally excited CO<sub>2</sub> with atomic O, where we are able to convert to the atmospherically relevant reaction via a known equilibrium constant. The goal of this experiment was to measure the magnitudes of rate coefficients for vibrational energy states above the first excited state, a bending mode in CO<sub>2</sub>.

An isotope of CO<sub>2</sub>, <sup>13</sup>CO<sub>2</sub>, was used for experimental ease. The rate coefficients for given vibrational energy transfers in <sup>13</sup>CO<sub>2</sub> are not significantly different from <sup>12</sup>CO<sub>2</sub> at this level of precision. A slow-flowing gas mixture was flowed through a reaction cell: <sup>13</sup>CO<sub>2</sub> (vibrational specie of interest), O<sub>3</sub> (atomic O source), and Ar (bath gas). Transient diode laser absorption spectroscopy was used to monitor the changing absorption of certain vibrational modes of <sup>13</sup>CO<sub>2</sub> after a UV pulse from a Nd:YAG laser was fired. Ozone absorbed the UV pulse in a process which vibrationally excited <sup>13</sup>CO<sub>2</sub> and liberated atomic O. Transient absorption signals were obtained by tuning the diode laser frequency to an appropriate  $\nu_3$  transition and monitoring the population as a function of time following the Nd:YAG pulse. Transient absorption curves were obtained for various O atom concentrations to determine the rate coefficient of interest. The rotational states of the transitions used for detection were difficult to identify, though their short re-equilibration timescale made the identification irrelevant for vibrational energy transfer measurements. The rate coefficient for quenching of the (10<sup>0</sup>0) state was found to be  $(4 \pm 8) \times 10^{-12} \text{ cm}^3 \text{ s}^{-1}$  which is the same order of magnitude as the lowest-energy bend-excited mode:  $(1.8 \pm 0.3) \times 10^{-12} \text{ cm}^3 \text{ s}^{-1}$ . More data is necessary before it can be certain that the numerical difference between the two is real.

## I. INTRODUCTION

The planets Venus and Mars have been known to us since at least the second millennium B.C.E., though it has not been until recently that we have been able to understand their atmospheres.<sup>2,3</sup> Both planets are enveloped by atmospheres composed mostly of carbon dioxide (CO<sub>2</sub>). Venus contains a 96.5% CO<sub>2</sub> atmosphere with a surface pressure of 90atm; Mars a 95% CO<sub>2</sub> atmosphere with 0.007atm surface pressure.<sup>3,4</sup> Compare this with Earth's atmosphere of 0.035% CO<sub>2</sub> and 1atm surface pressure.<sup>3</sup> Within the past quarter century it has been determined that vibrational energy transfer (VET) between CO<sub>2</sub> and atomic oxygen (O) is involved with cooling processes found in the Martian, Venusian and Terrestrial atmospheres.<sup>5-7</sup> This process is especially important in regions not in local thermodynamic equilibrium (LTE), namely Earth's upper mesosphere/lower thermosphere.<sup>5</sup> In different planetary atmospheres this phenomenon occurs at different altitudes: Mars 115-145km, Venus peaks at about 125km and Earth 80-110km.<sup>5-8</sup> The cooling process proceeds as follows: a high kinetic energy (KE) oxygen atom collides with a vibrational ground state CO<sub>2</sub> molecule, the CO<sub>2</sub> is excited into a bend vibrational ( $v_2$ ) state robbing the oxygen of some of its KE, the CO<sub>2</sub> then relaxes back to its ground state by emission of 15 $\mu$ m IR radiation which results in a net cooling of that volume of air.<sup>5-7,12</sup> The aforementioned VET is noted below:



For triatomic molecules vibrational modes can be represented by ( $v_1 v_2^l v_3$ ), where  $v_1$  corresponds to the symmetric stretch mode,  $v_2$  bend mode,  $v_3$  asymmetric stretch mode.<sup>12</sup> The  $l$  superscript in  $v_2^l$  corresponds to the angular momentum associated with the bending modes of the molecule. The efficiency (rate coefficient) of the CO<sub>2</sub>-O energy transfer is necessary for accurate atmospheric modeling and can be determined experimentally for a given set of conditions. For ease in the laboratory the rate coefficient is determined from the reverse of what occurs in the atmosphere, namely:



That is in the lab, de-excitation of a  $v_2$  excited  $\text{CO}_2$  by atomic O is used and can be appropriately translated to the atmospherically relevant reaction using a known equilibrium constant,  $K$ :

$$k_1/k_{-1} \equiv K = 2e^{-\Delta/kT}$$

where  $k_1$  is the atmospheric  $\text{CO}_2$ -O VET and  $k_{-1}$  is the lab-based VET,  $T$  is temperature in Kelvin,  $k$  is Boltzmann's constant and  $\Delta$  is the energy difference in wavenumber ( $\text{cm}^{-1}$ ) between the higher and lower state in the VET. At  $T = 296\text{K}$  for the  $(00^0_0) - (01^1_0)$  transition in  $^{13}\text{CO}_2$  ( $\Delta = 648.5\text{cm}^{-1}$ ) the equilibrium constant is 0.44.<sup>5</sup>

This specific bend vibrational state is the lowest energy excited state in  $\text{CO}_2$  and therefore the most likely to be populated by collisional energy transfer and thus involved in thermal atmospheric dynamics. This rate coefficient has been measured by the Castle group at room temperature and over a range of temperatures relevant to Earth's mesosphere and lower thermosphere (unpublished data, Castle group).<sup>5</sup> Vibrational energy transfer between O and higher energy excited states of  $\text{CO}_2$  (*e.g.* symmetric stretch  $v_1$ , asymmetric stretch  $v_3$  and combinations & overtones of the three vibrational modes), though auxiliary to the effects of the lowest energy bend state, may still contribute significantly to atmospheric cooling.<sup>4,12</sup> Due to their lessened abundance, however, the rate coefficients governing these vibrational energy transfers are even less well known, if at all, than those of the first bend-excited state both in magnitude and atmospheric importance. Our goal in this experiment was to begin to determine the efficiencies (rate coefficients) for vibrational quenching of these higher-energy states by atomic oxygen.

## II. MATERIALS & METHODS

### a) $^{13}\text{CO}_2$

The use of  $^{13}\text{CO}_2$  over  $^{12}\text{CO}_2$  was done as a matter of experimental convenience. In theory, rate coefficients for identical VETs in  $^{13}\text{CO}_2$  and  $^{12}\text{CO}_2$  should be similar, and our laboratory measurements agree with this (unpublished data, Castle group). The use of an isotopically pure sample of  $^{13}\text{CO}_2$  avoids the interference of ambient lab  $^{12}\text{CO}_2$  vibrations during the course of diode laser spectroscopy (discussed later). Additionally the use of  $^{13}\text{CO}_2$  allows for temperature dependent data to be taken within the range of our diode laser's output, 2220-2280 $\text{cm}^{-1}$ . Also the ratio of  $^{12}\text{C}/^{13}\text{C}$  on Earth, Venus and Mars is about 90, and for the  $\text{CO}_2$  rich atmospheres of Mars and Venus this means a larger mixing ratio of  $^{13}\text{CO}_2$  compared with that of Earth's atmosphere, therefore a more applicable scenario for the specific  $^{13}\text{CO}_2$  VETs.<sup>9,10</sup>

## **b) Experiment<sup>5</sup>**

A 1-m Al reaction cell of inner diameter (ID) 2.54cm, capped with sapphire cell windows was used in this experiment. Gases were slowly flowed through the cell during data collection via four 0.48cm ID Teflon tubes spaced equally about the cell end. Total gas pressure within the cell was measured with an MKS Baratron capacitance manometer and maintained via a throttled roughing pump with typical values being on the order of 10torr. The gases' partial pressures, save for  $\text{O}_3$ , were taken to be proportional to their individual mass flow rates, controlled via MKS MassFlo flow controllers with typical values of 0.10-0.14 standard  $\text{atm cm}^{-3} \text{ min}^{-1}$  (sccm)  $^{13}\text{CO}_2$  and 30.0-50.0sccm Ar. Argon acted as a bath gas: quenching electronically excited atomic-O atoms resulting from  $\text{O}_3$  photolysis (discussed later) as well as allowing for the modulation of the net cell pressure. Ozone at partial pressures 5-200 mtorr was introduced into the cell through a needle valve. Ozone concentrations were measured using a photomultiplier tube (PMT) which detected intensity levels of 120Hz sinusoidal, 254nm UV emission from an Hg-lamp; intensity levels with and without  $\text{O}_3$  present allowed its partial pressure to be determined. Ozone was made by passing  $\text{O}_2$  through an ozonator (Ozomax) and was stored on a silica gel column at  $-65^\circ\text{C}$ .

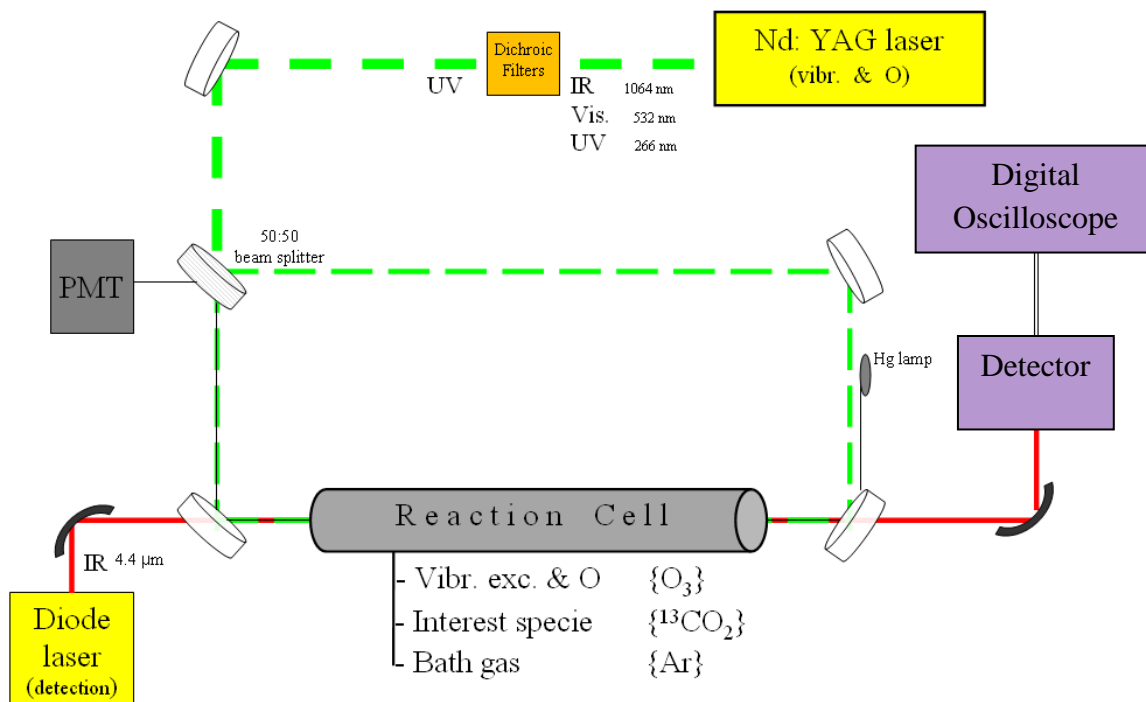


**Figure 1** A schematic of our experimental setup. The reaction cell contained a mixture of slow-flowing gases composed of O<sub>3</sub> which provided atomic O after YAG photolysis, <sup>13</sup>CO<sub>2</sub> our specie of interest, and Ar bath gas which quenched electronically excited O and also acted as net pressure modulation in the cell. The Hg lamp was placed in the noted position only when O<sub>3</sub> concentration was being measured, otherwise it was removed from the YAG beam path. Other apparatus are discussed in the text.

A 266nm frequency-quadrupled Nd:YAG laser (Continuum Surelite) was used to induce a temperature jump in the cell. The geometry shown in Figure 1 was used. Dichroic filters placed early in the Nd:YAG beam-path act to minimize residual 1064nm and 532nm emission from reaching the cell. The 266nm radiation was split with a 50:50 dichroic beamsplitter and sent through both ends of the cell to reduce attenuation along its length. The Nd:YAG beam was overlapped with the diode beam (discussed next) and pulsed at 5.4Hz. Each YAG pulse acted to photolyse O<sub>3</sub> into O<sub>2</sub> and O, the latter acting to quench vibrationally excited <sup>13</sup>CO<sub>2</sub>.

The diode laser (Laser Components) used for transient diode laser absorption spectroscopy (TDLAS) was tuned to approximately 4.4μm and was detected using a liquid-nitrogen cooled InSb detector (Infrared

Associates). The diode acted to probe the  $^{13}\text{CO}_2$  vibrational populations by  $4.4\mu\text{m}$  absorption resulting in an added quantum of  $\nu_3$  vibration, Figure 2. The divergent diode beam was collimated for travel through the cell then focused onto the detector using parabolic mirrors as shown in Figure 3. To reduce extraneous light a  $3.0\text{-}5.0\mu\text{m}$  antireflection-coated Ge window was placed in front of the diode while a  $3.8\text{-}4.8\mu\text{m}$  band-pass filter (Janos Technology) was placed directly in front of the InSb detector. Two irises were used to confine the diode beam-width to be several times smaller than that of the Nd:YAG laser. For data collection the diode was tuned to the specific frequency of a vibrational state of interest and that population was then monitored as a function of time after the Nd:YAG pulse, generating a transient absorption curve, Figure 4.

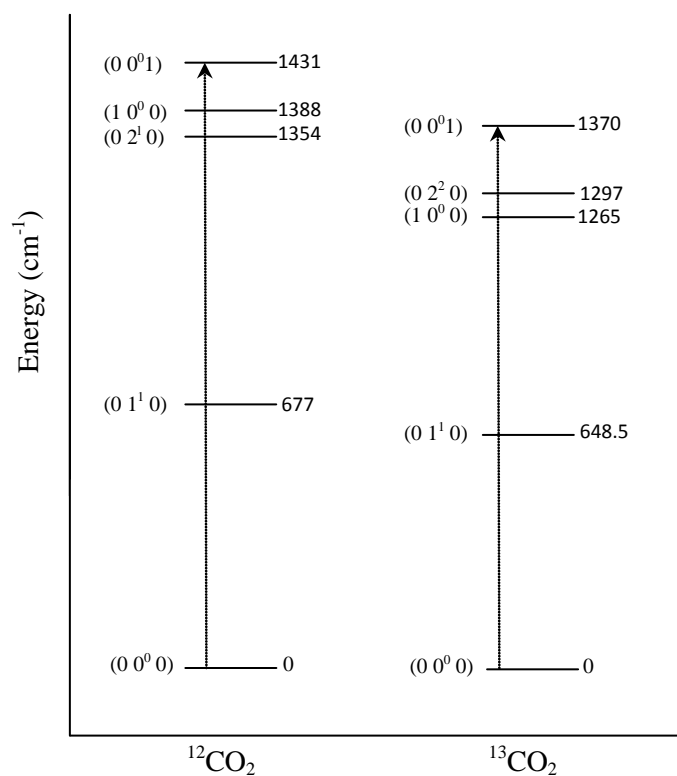


**Figure 2** Lowest vibrational energy levels of  $^{12}\text{CO}_2$  and  $^{13}\text{CO}_2$ , with energy above ground state  $(00^00)$  given in wavenumbers ( $\text{cm}^{-1}$ ). Representative diode absorption transitions are shown by the dashed arrows,  $(00^00)$  to  $(00^01)$ , this specific transition was not used in experimentation. For experimental data the  $(10^00)$  to  $(10^01)$  transition was used.<sup>11,13</sup>

From the InSb detector the data was passed through a preamplifier before being read, averaged (~500) and stored on a digital oscilloscope (LeCroy Wavesurfer). Each transient absorption curve represents 10,000 data points and typically eight different curves are obtained in a data set to determine the rate coefficient.

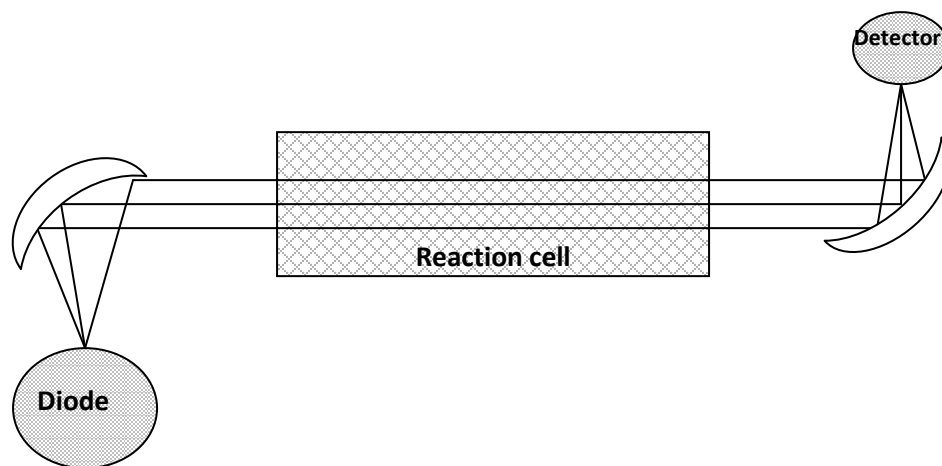


**Figure 3** A schematic of the divergent diode beam being collimated then focused by parabolic mirrors.

### c) Peak Identification

Rotational states equilibrate on timescales much shorter than those of vibrational states, therefore specific rotational identification of peaks is not necessary for determination of vibrational state dynamics. Any rotational state within the vibrational band of interest would yield the same results for the vibrational relaxation rate coefficient. Though for specific rotational and vibrational identification observed rovibrational spectra could be compared with those from the high-resolution transmission (HITRAN) database. HITRAN is a database of experimentally measured emission line positions and intensities for molecules of atmospheric importance.<sup>14</sup> Rovibrational identification is done by matching-up successively

higher energy levels between the HITRAN and observed spectrum until an unequivocal match is found, Figure 5.

A previously observed  $\nu_2$  region (K. Castle, unpublished data) was used as a starting region for observation. To determine identity of peaks on the rovibrational absorption spectrum of  $^{13}\text{CO}_2$ , pure  $^{13}\text{CO}_2$  was flowed into the cell in increasing amounts, 0.02-2.49sccm. Ground state,  $\nu_2$  and two higher energy transitions were clearly identified, Figure 6. The ground state and  $\nu_2$  excited state are the two lowest energy levels and therefore are be more intense than subsequent higher vibrational states. The exact rotational identity of the high-energy peaks were undetermined, though data was consistently taken on the ( $10^0$ ) peak, Figure 6.

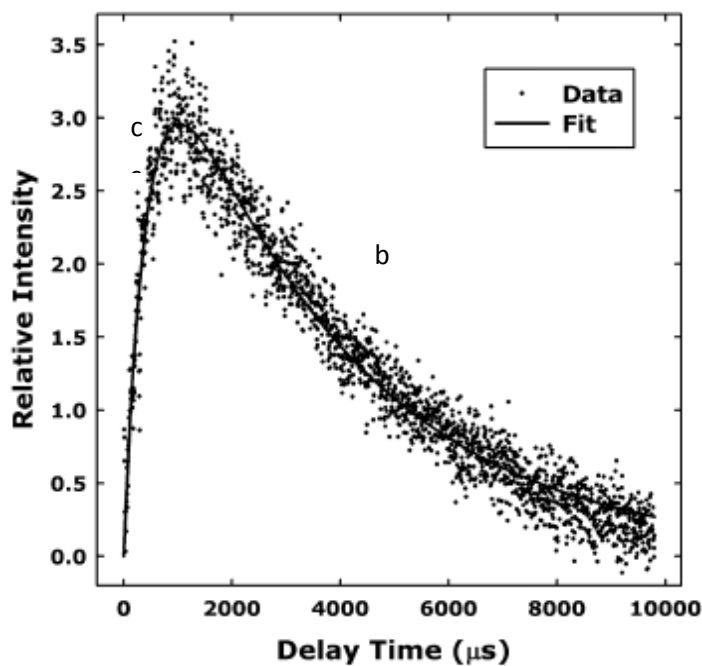


**Figure 4** A representative transient absorption curve for  $\text{CO}_2$  with double-exponential fit curve,  $I = a(e^{-bt} - e^{-ct})$ . The  $b$  and  $c$  parameters are shown on the graph, corresponding to the thermal reequilibration and quenching of  $\text{CO}_2$ , respectively. [Adopted from Castle *et al.*, 2006]

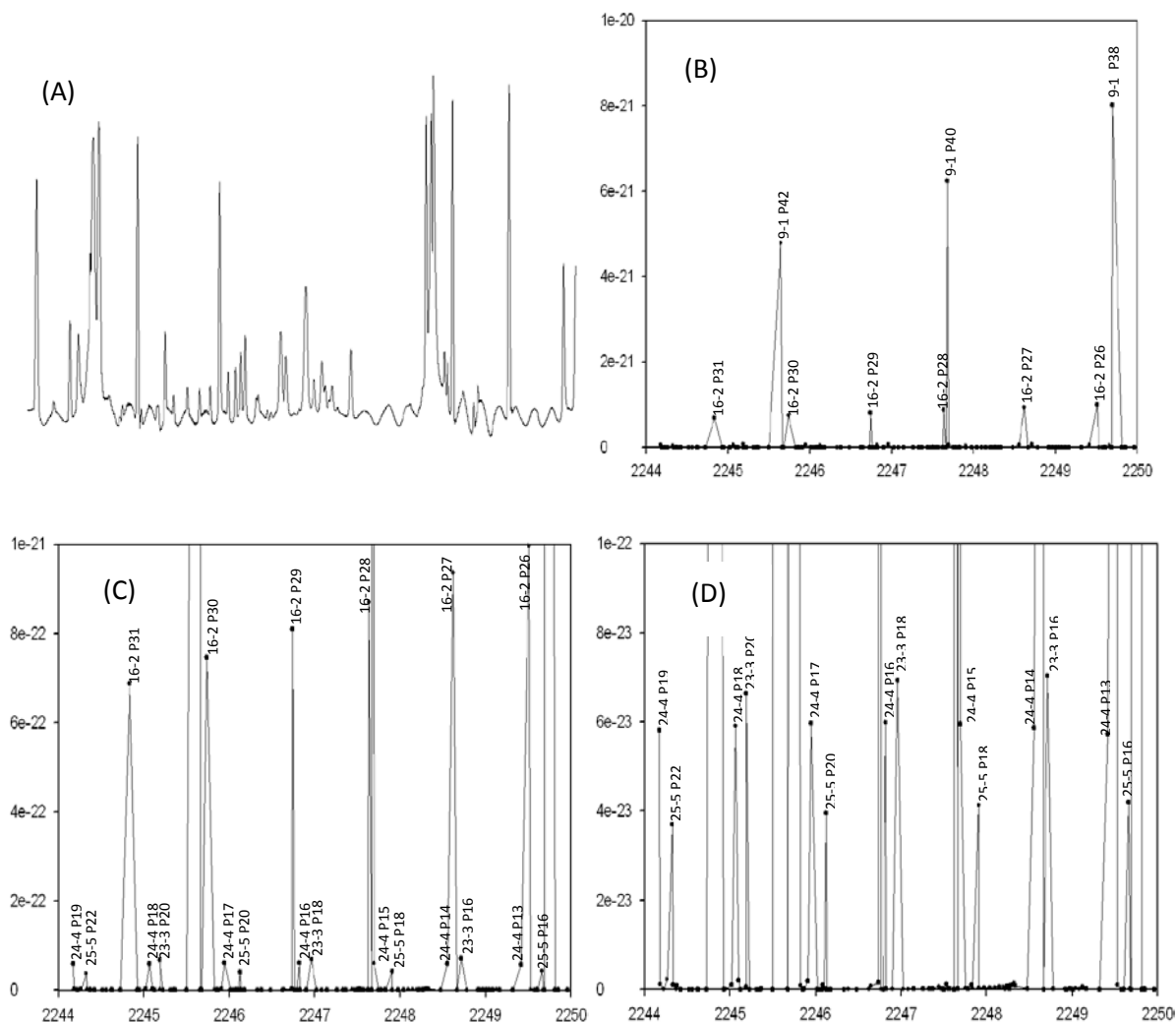


**Figure 5** A) Observed rovibrational spectrum for  $^{13}\text{CO}_2$  showing intensity as a function of wavenumber ( $\text{cm}^{-1}$ ). B)-D) HITRAN spectra showing intensity as a function of wavenumber, with the vertical intensity scale shrinking from B to D. Peaks are noted. The HITRAN notation shows the energy level ranking with the lowest energy at 1. It displays the ending state energy rank and beginning state energy rank. For our experiment the ending vibrational state is the same as the beginning with just a quantum of  $\nu_3$  added. For example 16-2 corresponds to the 2<sup>nd</sup> highest energy level being excited to the 16<sup>th</sup> highest energy level, or in other notation (01<sup>1</sup>0) going to (01<sup>1</sup>1). The rotational state is noted P#, where P denotes that the change of the rotational quantum number is  $\Delta J = -1$  and # is the rotational quantum number, J, of the initial state.<sup>13</sup>

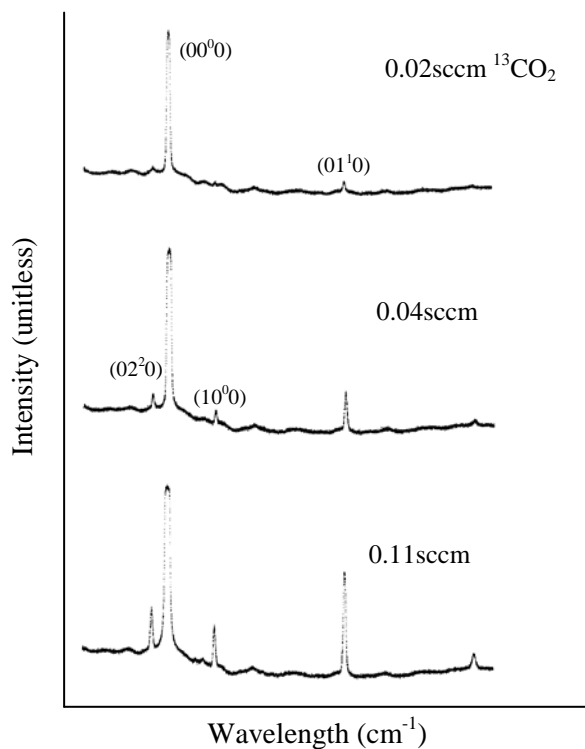


**Figure 6** Spectrum of  $^{13}\text{CO}_2$  in the  $2250\text{cm}^{-1}$  range (exact wavelengths undetermined), showing increasing higher energy rovibrational populations with increasing  $^{13}\text{CO}_2$  flow. The lowest two energy levels are shown,  $(00^0_0)$  and  $(01^1_0)$ . The third and fourth lowest levels are  $(10^0_0)$  and  $(02^2_0)$ , with data presented in this thesis being taken on the former. All peaks are  $\nu_3 \rightarrow \nu_3+1$  transitions with the starting state labeled for each peak.

#### d) Analysis

The resulting transient absorption curves, after subtracting off background, approximate the shape of a double exponential function, Equation 1:

$$I = a(e^{-bt} - e^{-ct}) \quad (1)$$

as shown in Figures 4 & 8. In Eq. 1  $I$  is the given intensity of diode signal as a function of time  $t$  after the Nd:YAG pulse. The  $a$  parameter is related to the maximum height of the fit, the  $b$  parameter to the decay rate of the fall (which physically corresponds to the temperature re-equilibration of the system back to its original temperature) and the  $c$  parameter to the rate of the rise (physically corresponding to the collisional quenching of  $\text{CO}_2$  by all species present). It is therefore the  $c$  parameter which we desire, and specifically, the change in the  $c$  parameter with varying concentrations of atomic oxygen, which allows for the distinction of  $\text{CO}_2$ -O and  $\text{CO}_2$ -M quenching, where M are other quenching species in the cell.

Due to the approximate nature of these measurements, transient curves were fit individually (SigmaPlot) using Eq. 1. After all  $c$  parameters had been determined they were plot as a function of O-atom concentration and this distribution was then linearly fit, Figure 7. The slope of this linear fit line gave the rate coefficient.

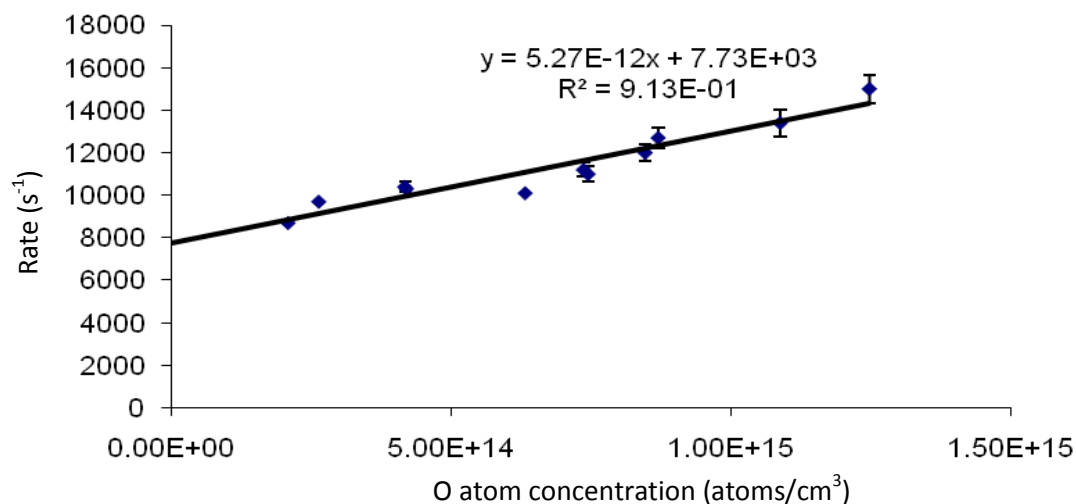


**Figure 7** Plot of  $(10^{00})$   $^{13}\text{CO}_2$ -O VET rate as a function of O atom concentration. The slope of the linear fit is the rate coefficient, namely:  $5.27 \times 10^{-12} \text{ cm}^3 \text{ s}^{-1}$ .

### III. RESULTS & DISCUSSION

We found the higher energy state, ( $10^0$ ), to have a quenching rate coefficient on the same order as the  $\nu_2$  state,  $(4 \pm 8) \times 10^{-12} \text{ cm}^3 \text{ s}^{-1}$  versus  $(1.8 \pm 0.3) \times 10^{-12} \text{ cm}^3 \text{ s}^{-1}$ , respectively.<sup>5</sup> It cannot be said with any statistical confidence whether this observed numerical difference is real or not. The rate coefficients for the  $\nu_2$  state determined in this experiment by our individual-fitting method matched the previously determined value from our lab,  $(2 \pm 4) \times 10^{-12}$  and  $(1.8 \pm 0.3) \times 10^{-12} \text{ cm}^3 \text{ s}^{-1}$  respectively, giving credence to our methodology of fitting.<sup>5</sup>

Uncertainties given are the result of previous study in the lab (unpublished testing) which showed interpersonal variation in this fitting method to generally vary the rate coefficient by no more than 100-200% the accepted value, though still remaining within the same order of magnitude. Therefore even with variations in this data fitting method, an answer of the proper order of magnitude should arise.

The excited state measured in this work is not directly coupled with the ground state. A further understanding of the energy cascade during higher energy vibrational quenching will be important in understanding their molecular dynamics as well as better understanding the true meaning of higher energy

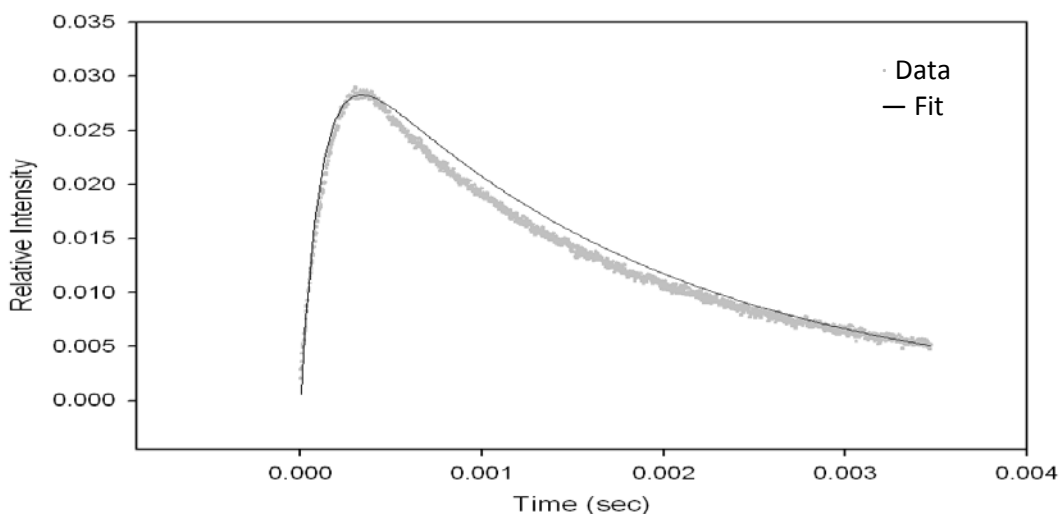


**Figure 8** Transient absorption signal from ( $10^0$ )  $^{13}\text{CO}_2$  data set at  $[\text{O}] = 2.10 \times 10^{14} \text{ atoms cm}^{-3}$ . Transients and fits at other O concentrations appeared similar in form. Fit using Eq. 1.

rate coefficients, for example: are there certain cascades preferentially used during vibrational quenching and how does this affect the possible repopulation of higher energy states? The complexity of the system is further magnified by the non-LTE conditions found in these atmospheric regions. Understanding the higher energy VETs will ultimately aid in more precise modeling of the atmospheres of Earth, Venus and Mars, especially for Venus as its dense, CO<sub>2</sub>-rich atmosphere and proximity to the Sun give it favorable conditions for significant population of these higher energy vibrational levels.

#### IV. BIBLIOGRAPHY

- <sup>1</sup> Sunset Boulevard. Dir. Billy Wilder. Paramount Pictures, 1950.
- <sup>2</sup> Leverington, David. Babylon to Voyager and Beyond: A History of Planetary Astronomy. Cambridge University Press, 2003: pp 1-5.
- <sup>3</sup> Lang, Kenneth R.. The Cambridge Guide to the Solar System. Cambridge University Press, 2003: pp 77-80.
- <sup>4</sup> Carroll, Bradley & Ostlie, Dale. An Introduction to Modern Astrophysics 2<sup>nd</sup> Ed. Pearson: Addison-Wesley, 2007: pp 742,767
- <sup>5</sup> Castle *et al.* (2006) Vibrational relaxation of CO<sub>2</sub> (v<sub>2</sub>) by atomic oxygen. Journal of Geophysical Research 111: A09303
- <sup>6</sup> López-Puertas & López-Valverde (1995) Radiative energy balance of CO<sub>2</sub> non-LTE infrared missions in the Martian atmosphere. Icarus 114, 113-129.

- <sup>7</sup> Keating & Bougher (1992) Isolation of major Venus thermospheric cooling mechanism and implications for Earth and Mars. Journal of Geophysical Research 97, 4189-4197.
- <sup>8</sup> Roldán, C. *et al.* (2000). Non-LTE Infrared Emissions of CO<sub>2</sub> in the Atmosphere of Venus. Icarus 47, 11-25
- <sup>9</sup> Wilquet, V. *et al.* (2008) Line parameters for the 01111–00001 band of <sup>12</sup>C<sup>16</sup>O<sup>18</sup>O from SOIR measurements of the Venus atmosphere. Journal of Quantitative Spectroscopy & Radiative Transfer 109, 895-905.
- <sup>10</sup> Moroz, V. I. (1998) Chemical composition of the atmosphere of Mars. Advances in Space Research 22(3), 449-457.
- <sup>11</sup> Dubost H. (1998) Picosecond to Minute Molecular Vibrational Dynamics in Cryosolids. Journal of Low Temperature Physics 111, 615-628.
- <sup>12</sup> Atkins, Peter & de Paula, Julio. Physical Chemistry 7<sup>th</sup> Ed.. W.H. Freeman and Company, 2002: pp 517-8, 520-523.
- <sup>13</sup> Personal correspondence, Karen Castle, 2010.
- <sup>14</sup> L. S. Rothman (1998) The HITRAN molecular spectroscopic database and HAWKS (HITRAN Atmospheric WorkStation): 1996 Edition. Journal of Quantitative Spectroscopy & Radiative Transfer 60(5), 665-710.